Electronic Supplementary Information

Preparation and Phase Transition of FeOOH Nanorods: Strain Effects on Catalytic Water Oxidation

Gisang Park, [§,a] Yong-Il Kim, [§,b] Young Heon Kim, [§,b] Mira Park,[c] Kyu Yeon Jang,[a] Hyunjoon Song[c,*] and Ki Min Nam[a,*]

[a] Department of Chemistry, Mokpo National University, Muan-gun, Jeonnam 1666 Yeongsan-ro, Cheonggye-myeon, Muan-gun, Jeonnam 58554, South Korea

E-mail: namkimin.chem@gmail.com

[b] Korea Research Institute of Standard and Science (KRISS), Daejeon 305-340, South Korea

[c] Department of Chemistry, Korea Advanced Institute of Science and Technology (KAIST), 291 Daehak-ro, Yuseong-gu, Daejeon 34341, South Korea

E-mail: hsong@kaist.ac.kr

[§] These authors contributed equally to this work.

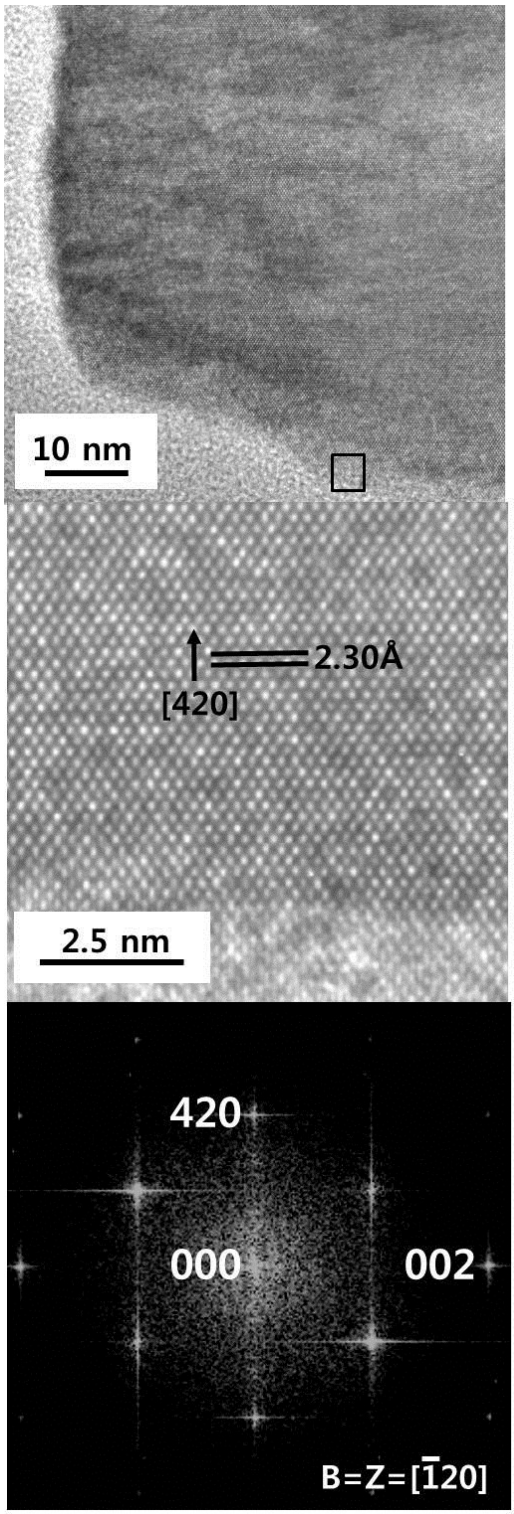

Fig. S1 HRTEM image and FFT measurement of β-FeOOH (A100) nanorod.

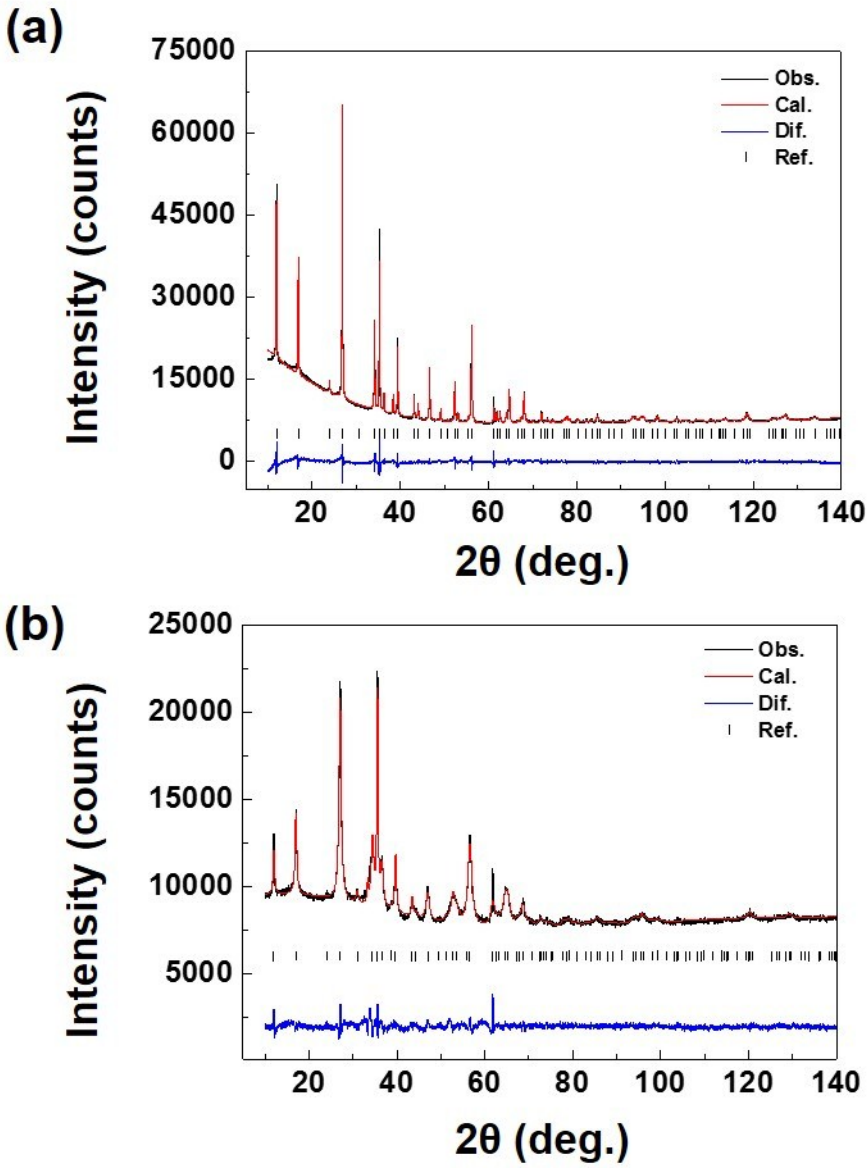

Fig. S2 Rietveld refinement patterns of (a) A200, and (b) A250 using X-ray powder diffraction data.

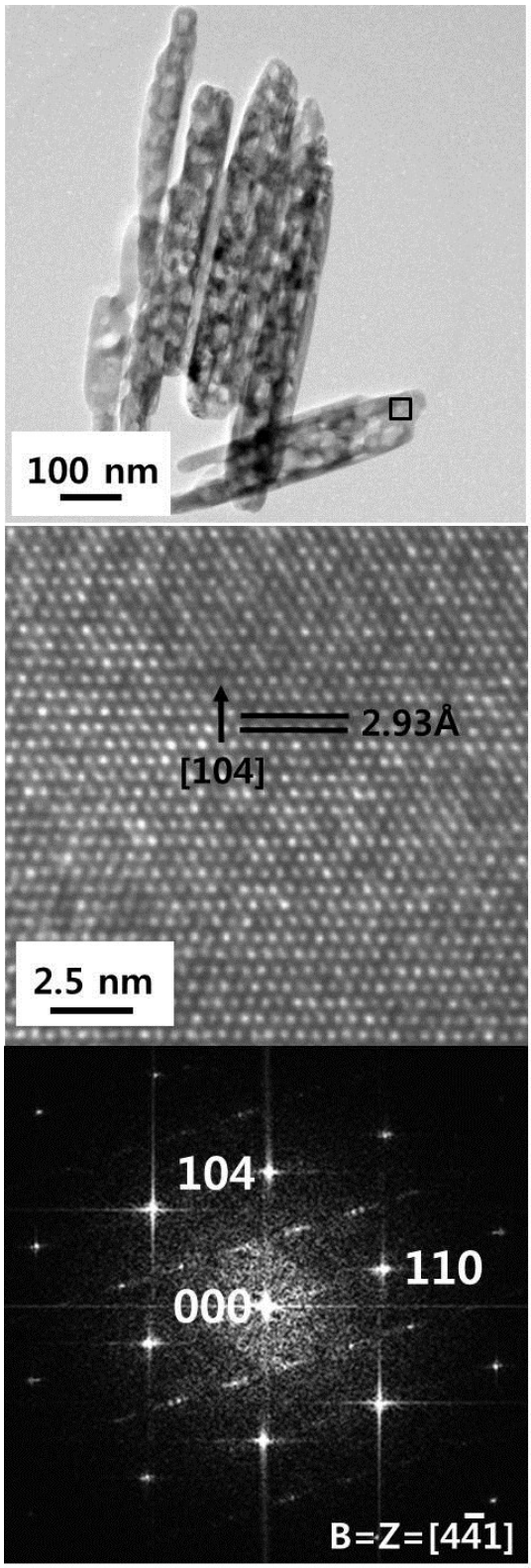

Fig. S3 TEM image and FFT measurement of A500 sample.

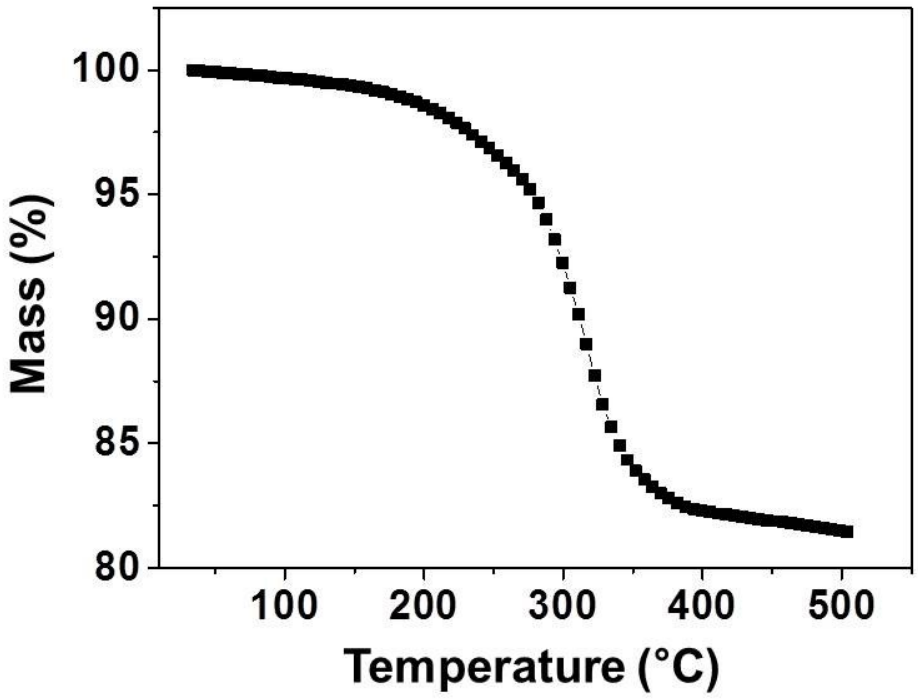

Fig. S4 TGA curve of β-FeOOH nanorods.

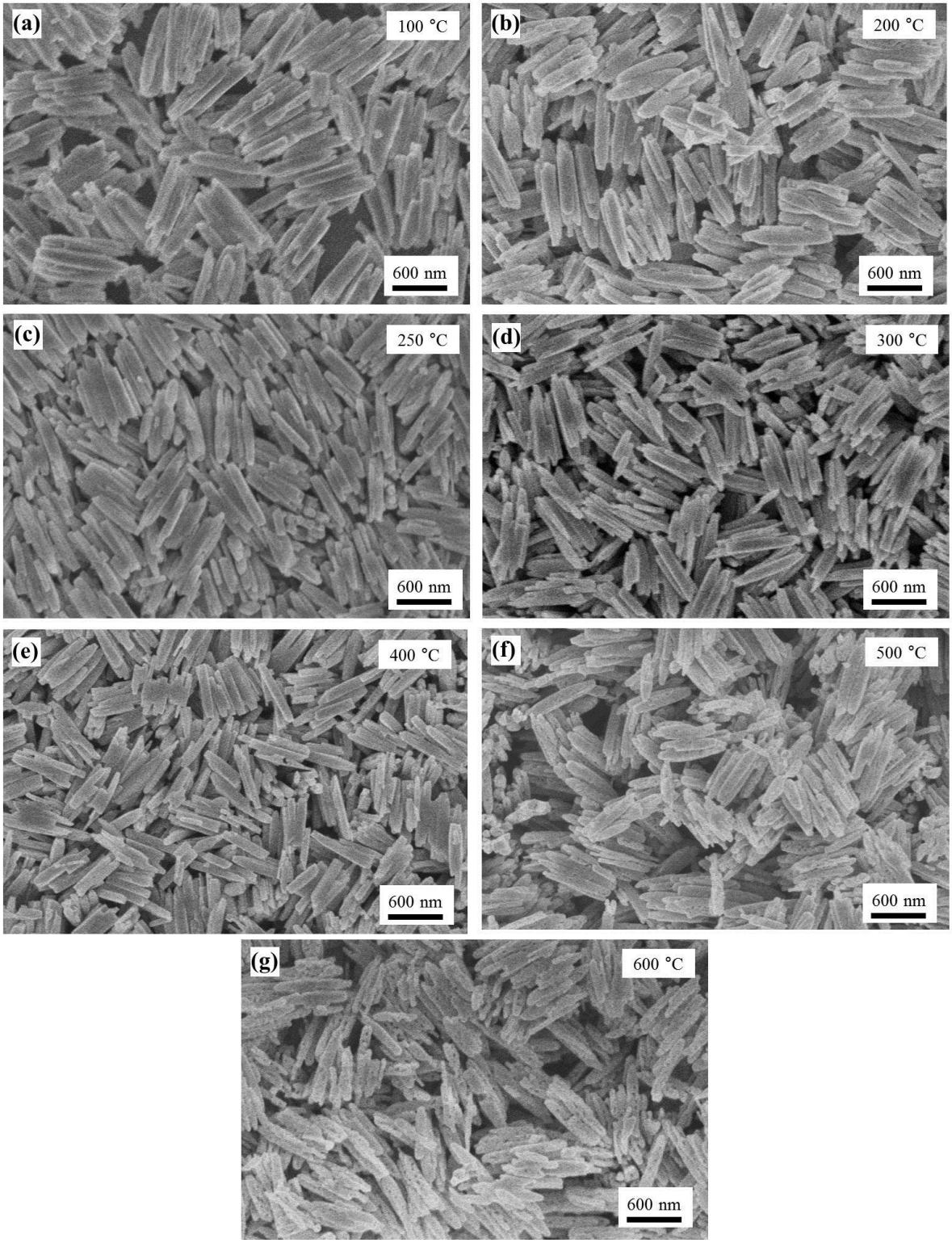

Fig. S5 SEM images of β-FeOOH nanorods with various thermal treatments in air. (a) β-FeOOH before thermal treatment, (b) samples after 200, (c) 250, (d) 300, (e) 400, (f) 500, (g) 600 °C thermal treatment.

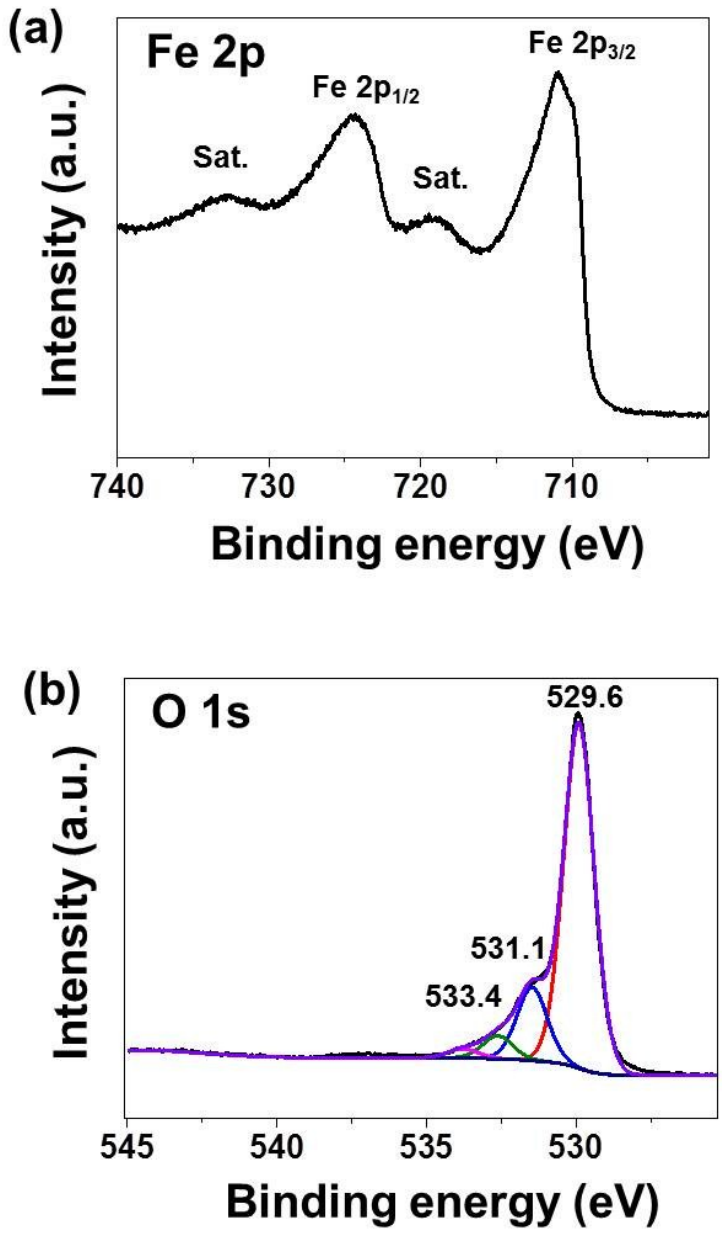

Fig. S6 High resolution XPS in the (a) Fe 2p, and (b) O 1s regions for Fe_2O_3 (A500) electrode.

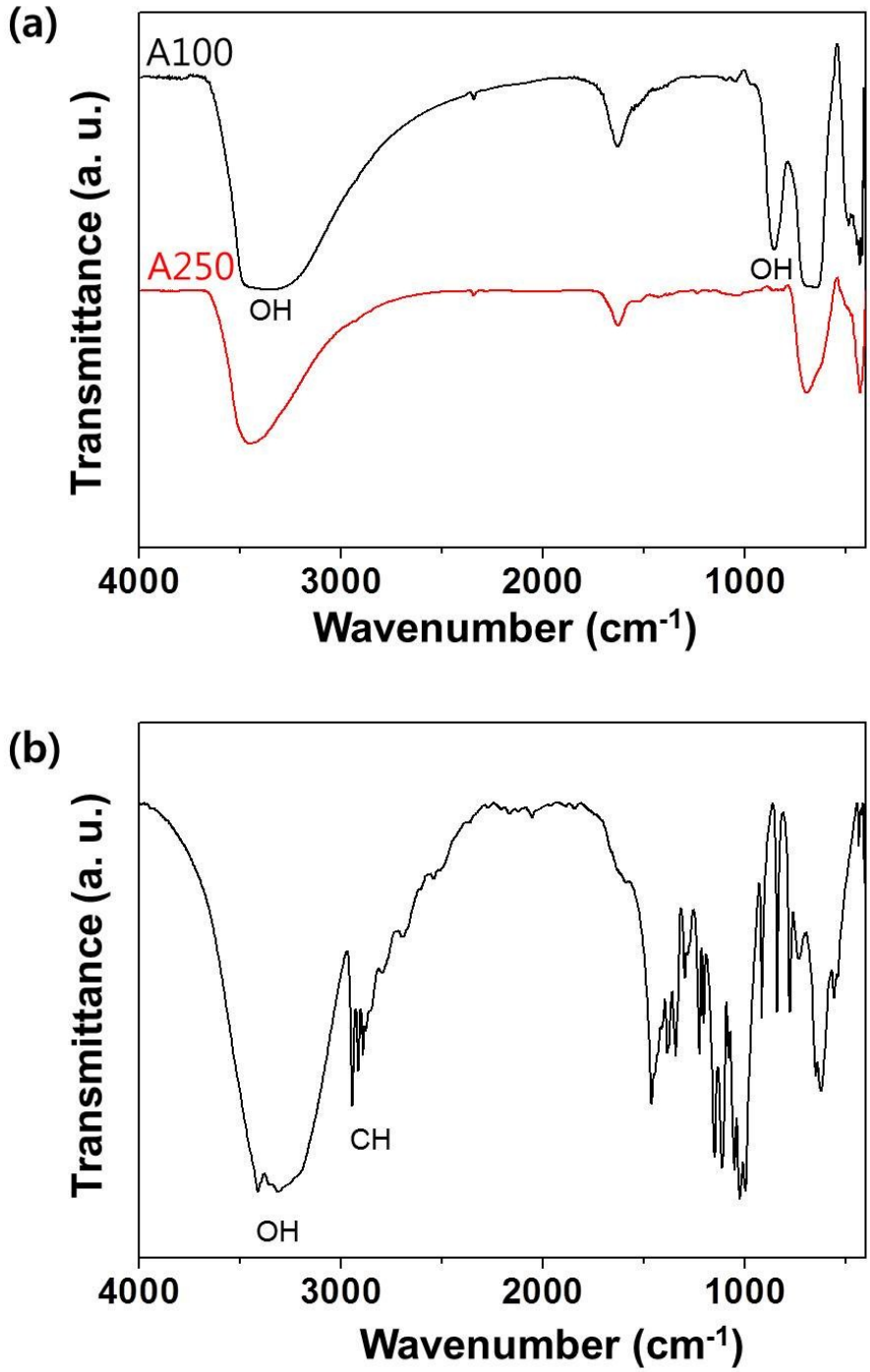

Fig. S7 FTIR spectra of the (a) β-FeOOH (A100) and strained-FeOOH (A250), and (b) glucose.

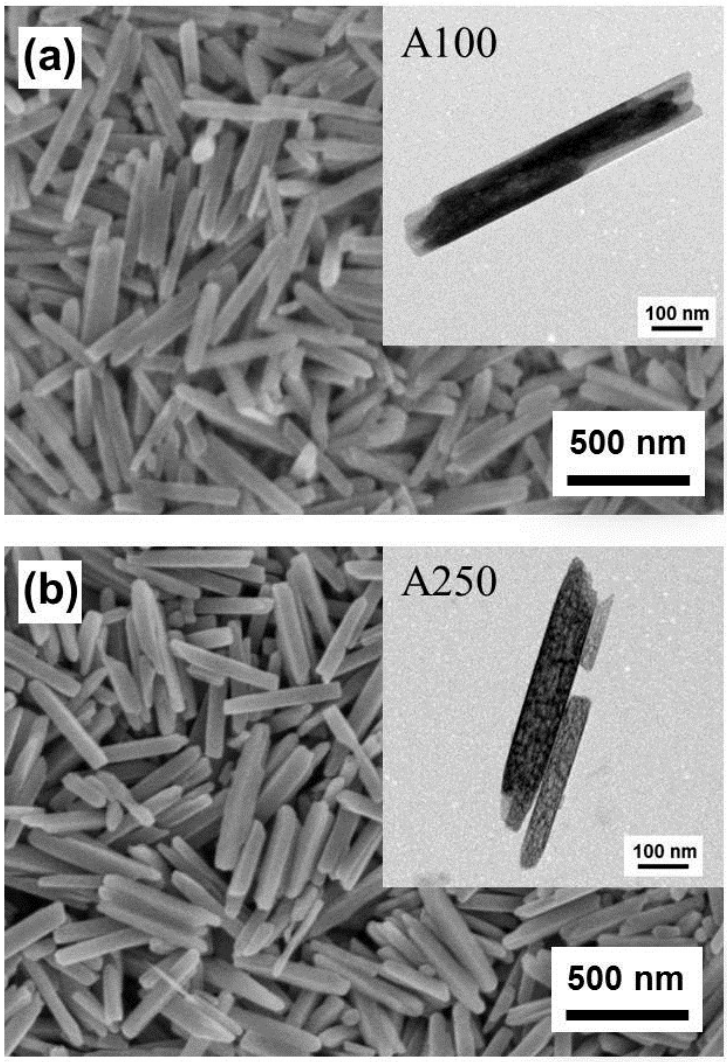

Fig. S8 SEM and TEM images (inset) of (a) A100 and (b) A250 prepared directly grown on a FTO substrate.

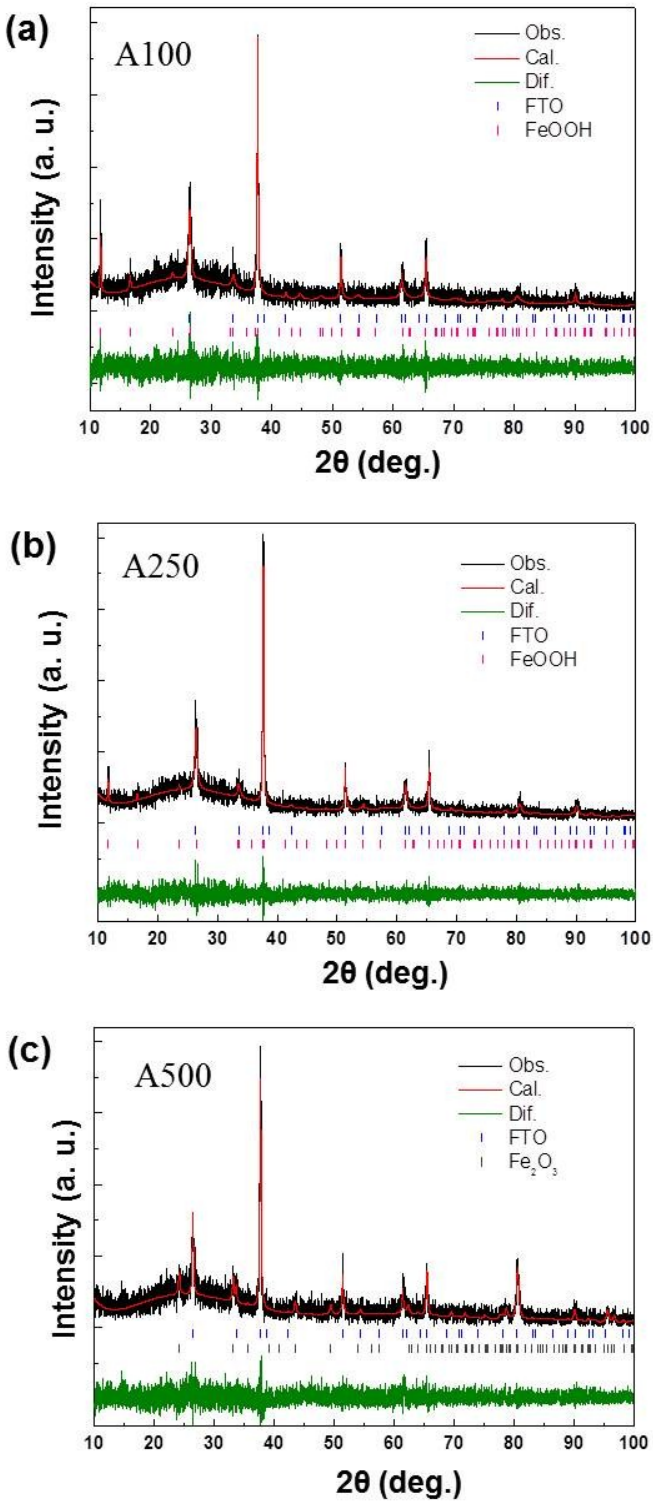

Fig. S9 XRD patterns of FeOOH nanorods on FTO substrate with typical thermal treatment for 3 h in air. (a) β-FeOOH (A100), and the sample thermally treated at (b) 250 °C (A250) and (c) 500 °C (A500) thermal treatment on FTO.

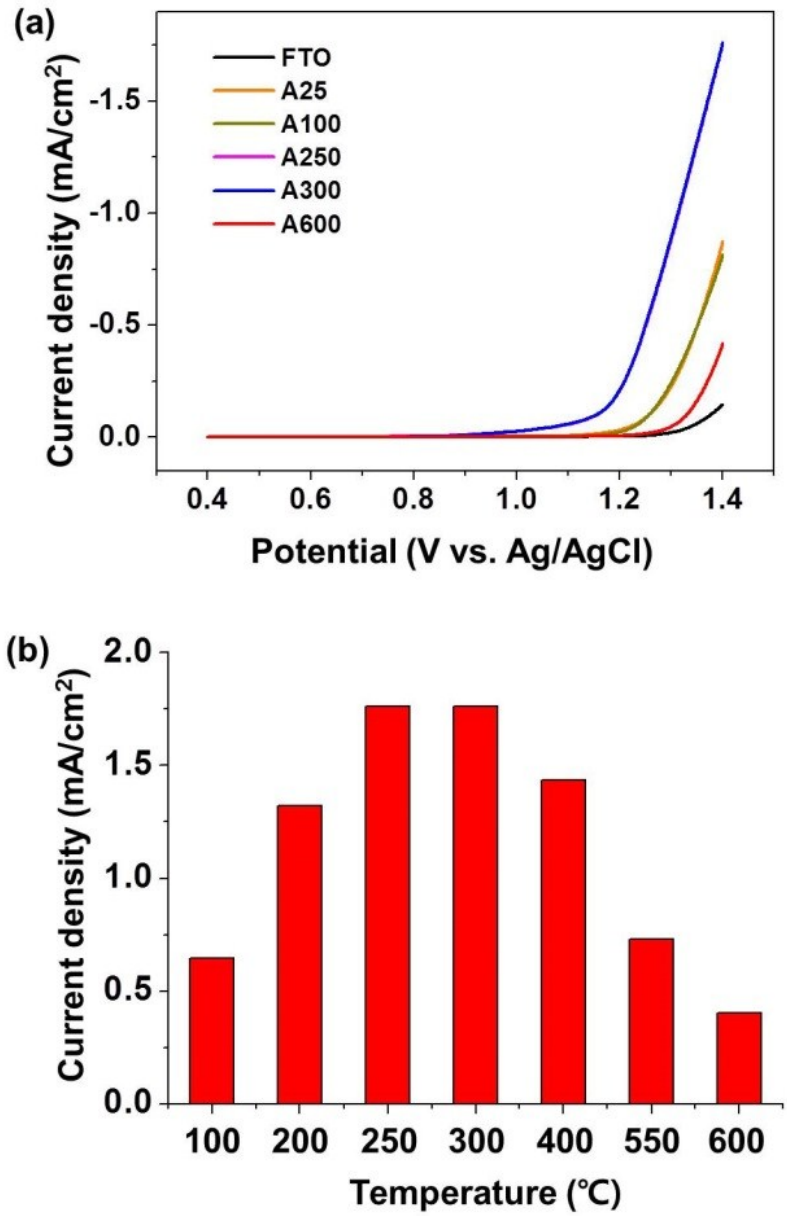

Fig. S10 (a) LSVs of β-FeOOH (A25, A100), strained-FeOOH (A250, A300), and Fe_2O_3 (A600) electrodes in phosphate buffer (pH 7), and (b) current density with the different heat treatment between 100 °C and 600 °C at an applied potential of 1.4 V versus Ag/AgCl.

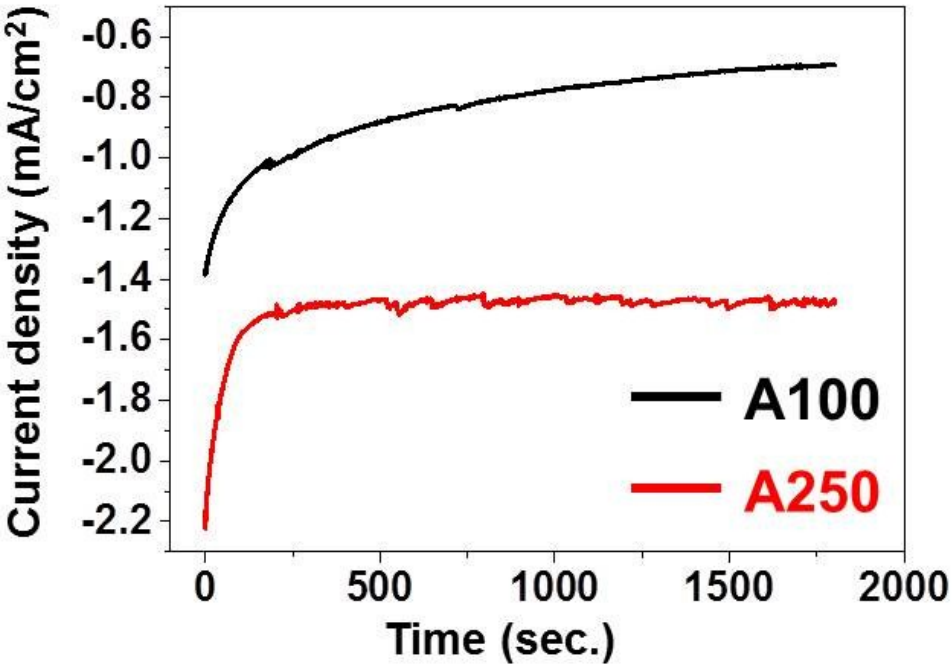

Fig. S11 Current-time response curve of A100 and A250 at an applied potential of 1.5 V vs Ag/AgCl in a phosphate buffer (pH 7).

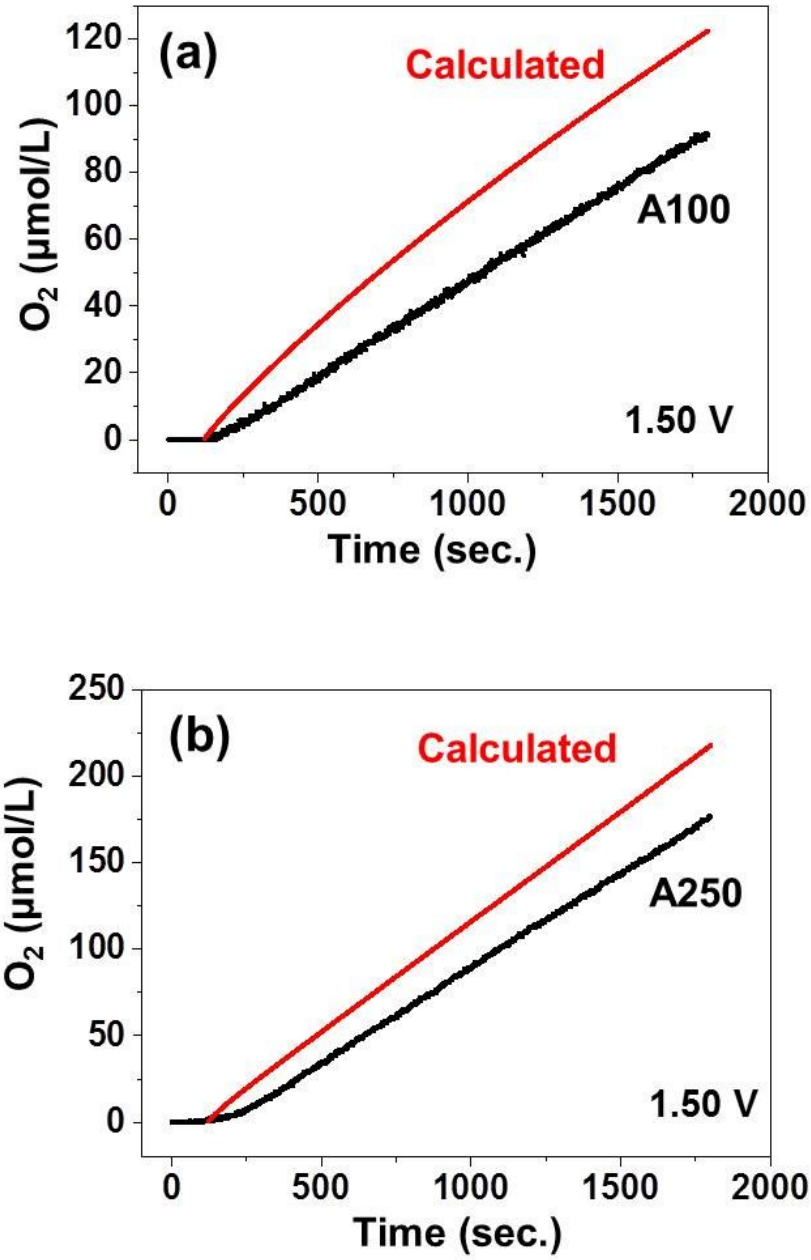

Fig. S12 Faradaic efficiency of A100 and A250 electrodes at an applied potential of 1.50 vs Ag/AgCl in a phosphate buffer (pH 7).

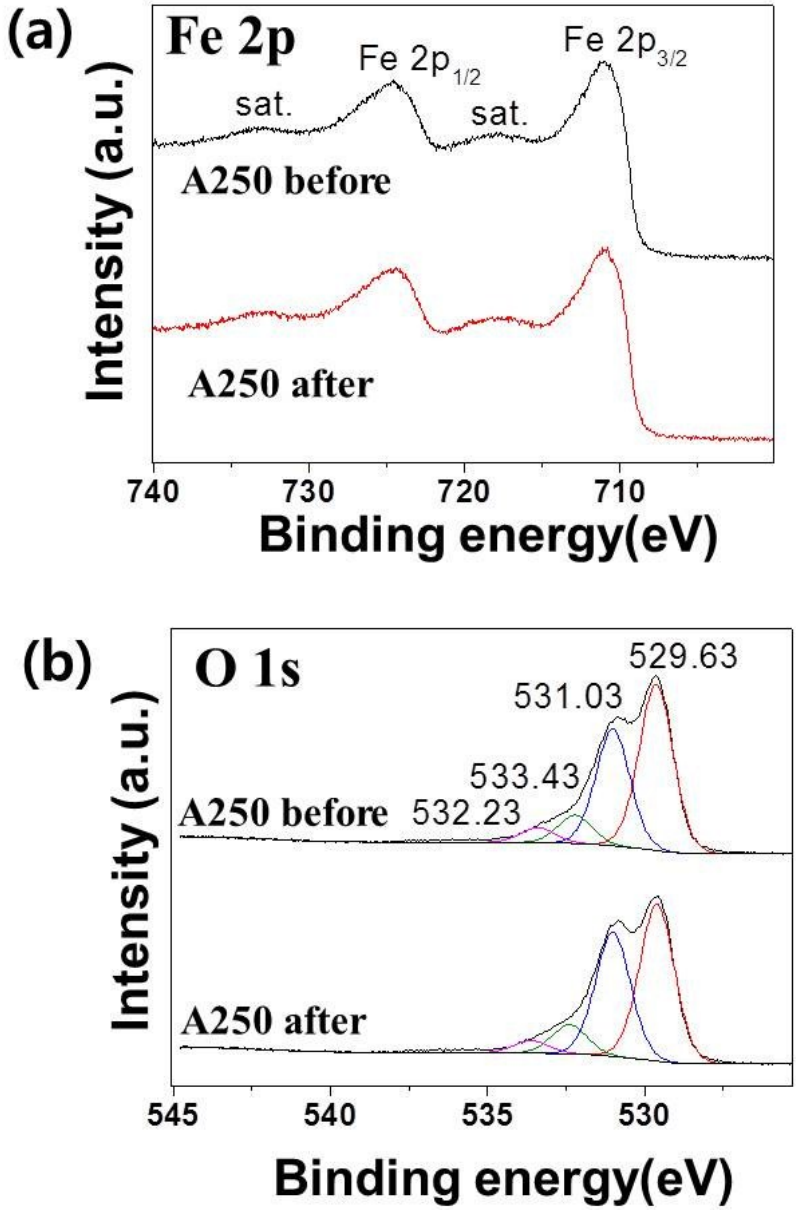

Fig. S13 High resolution XPS in the (a) Fe 2p, and (b) O 1s regions for strained-FeOOH (A250) electrodes before and after catalytic reactions.

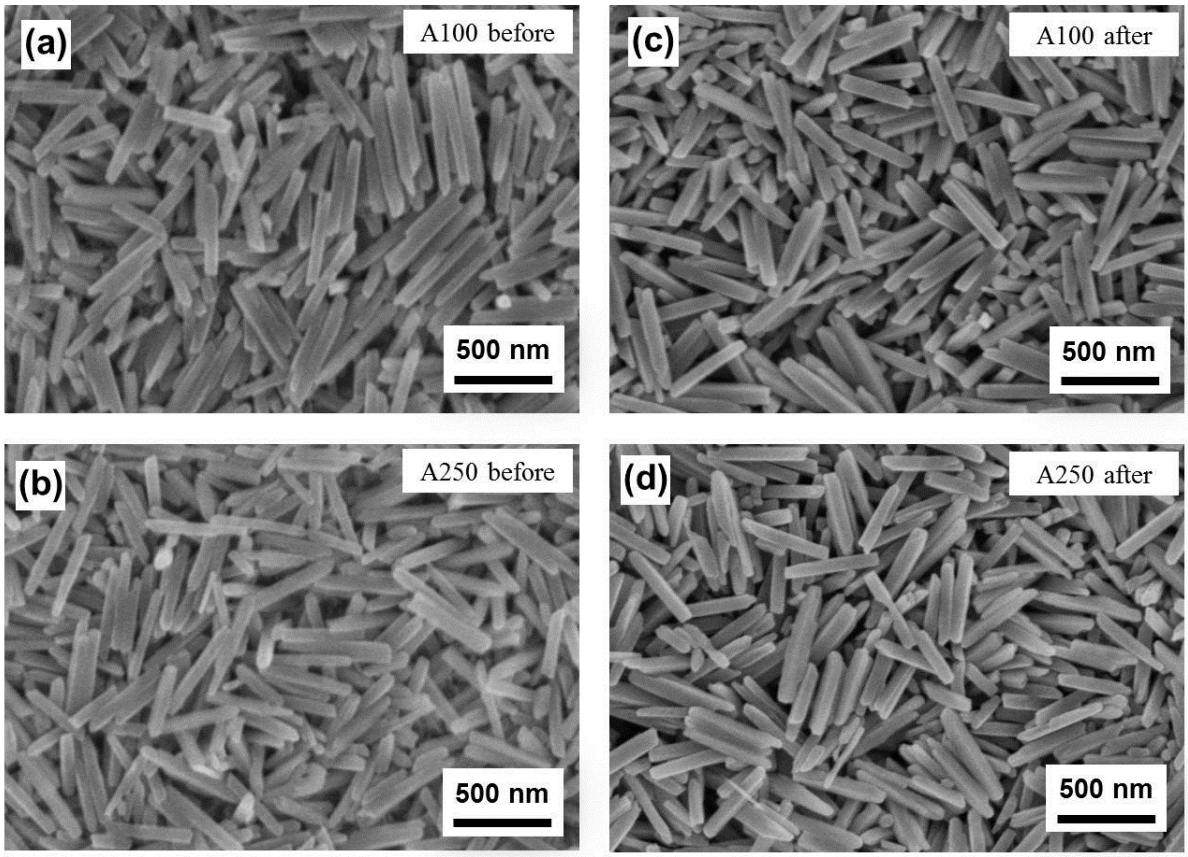

Fig. S14 SEM images of (a) A100/FTO and (b) A250/FTO, and (c) A100/FTO and (d) A250/FTO after the catalytic reaction.

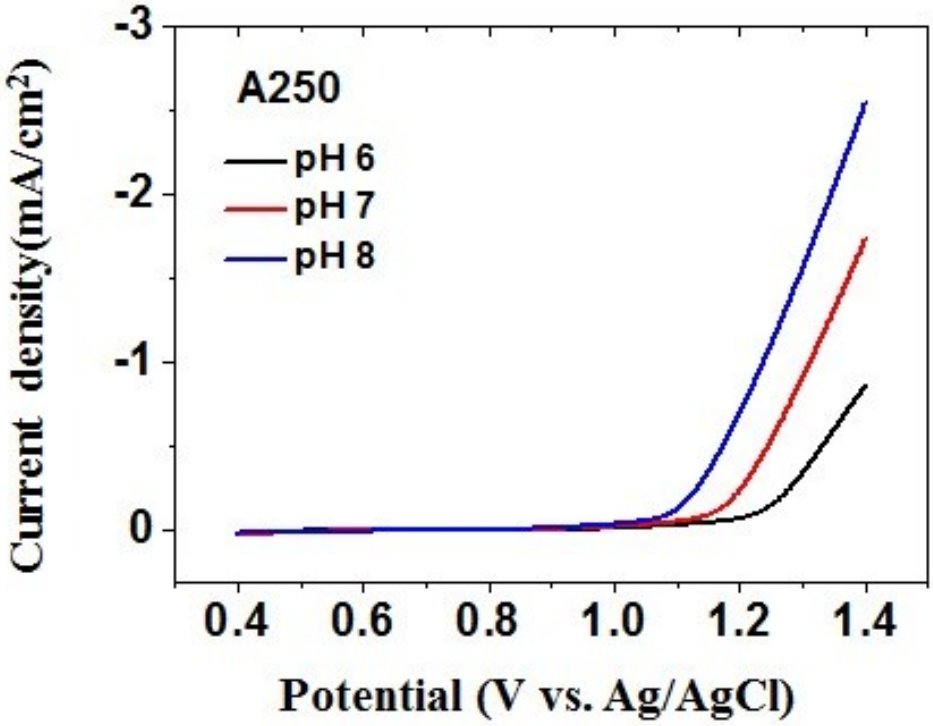

Fig. S15 LSVs of A250 electrode depends on pH in phosphate buffer solutions.

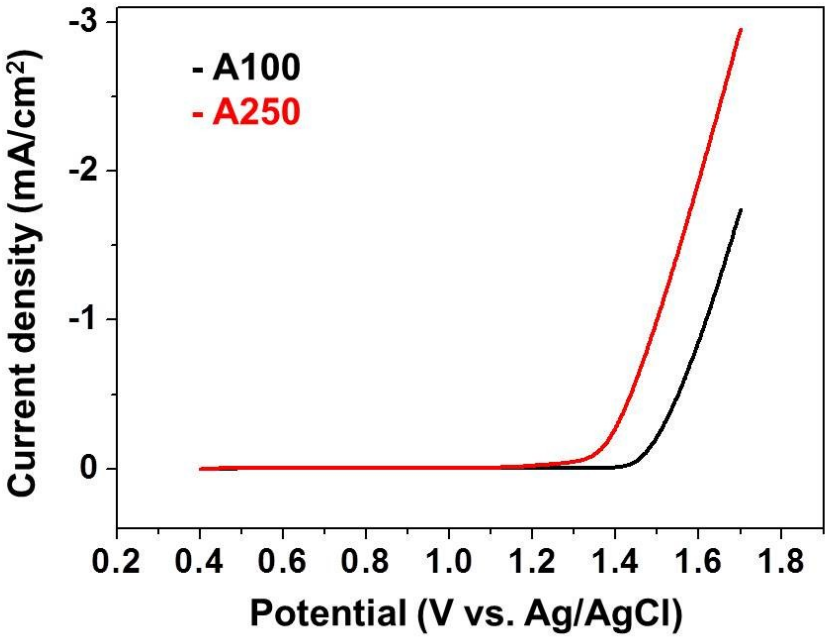

Fig. S16 LSVs of β-FeOOH (A100), and strained-FeOOH (A250) in 0.1 M NaCl solution. Scan rate of 20 mV/s.

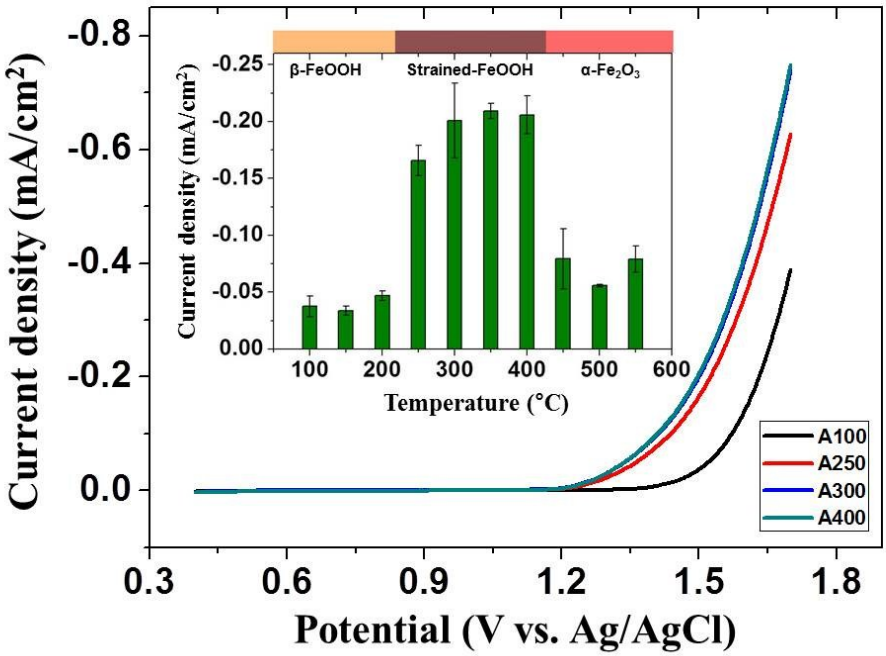

Fig. S17 LSVs of β-FeOOH (A100) and strained-FeOOH (A250, A300, A400) electrodes in phosphate buffer (pH 7), and current density with the different heat treatment between 100 ^{o}C and 600 ^{o}C at an applied potential of 1.5 V versus Ag/AgCl (inset).

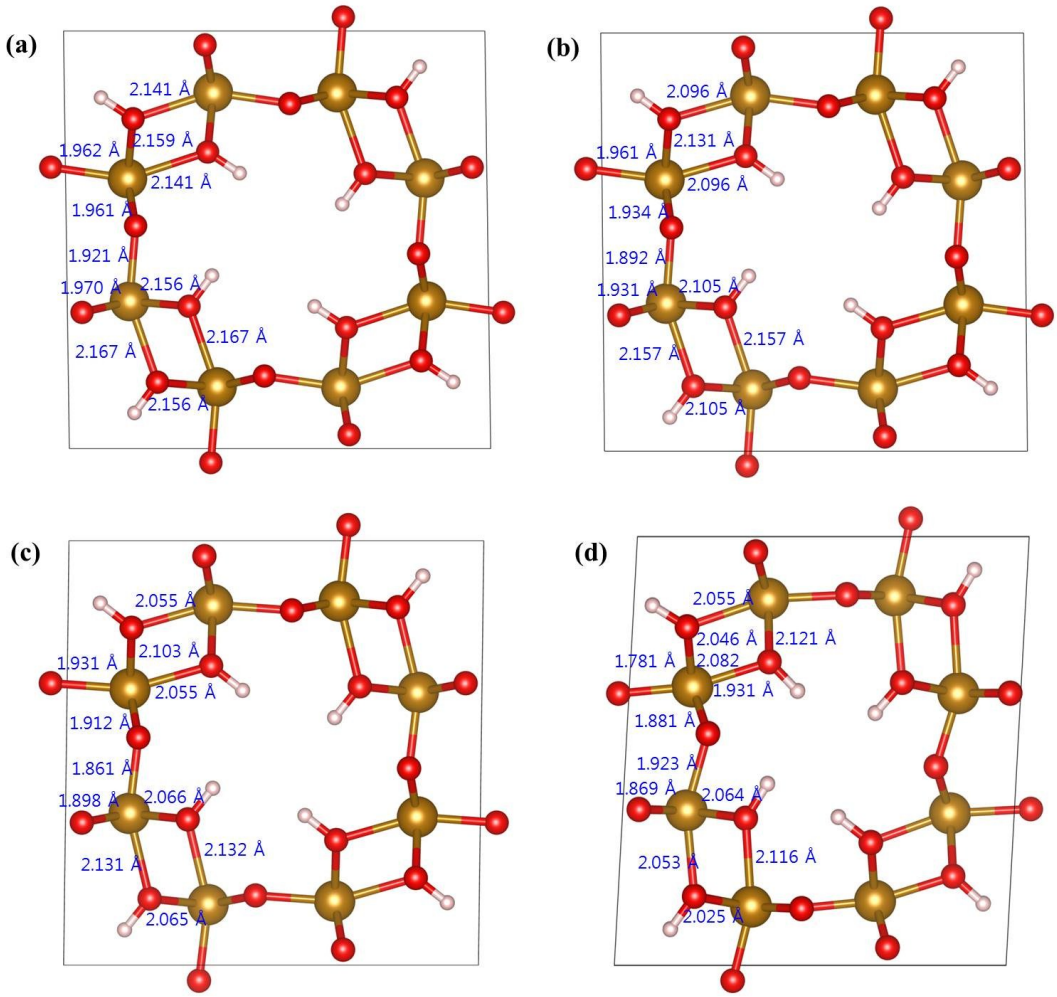

Fig. S18 The local environment of the Fe and O atoms at the crystal structure of (a) β-FeOOH after the stabilization. Bonding geometry of Fe and O atoms after (b) one electron, (c) two electrons, (d) three electrons extraction from the β-FeOOH structure.

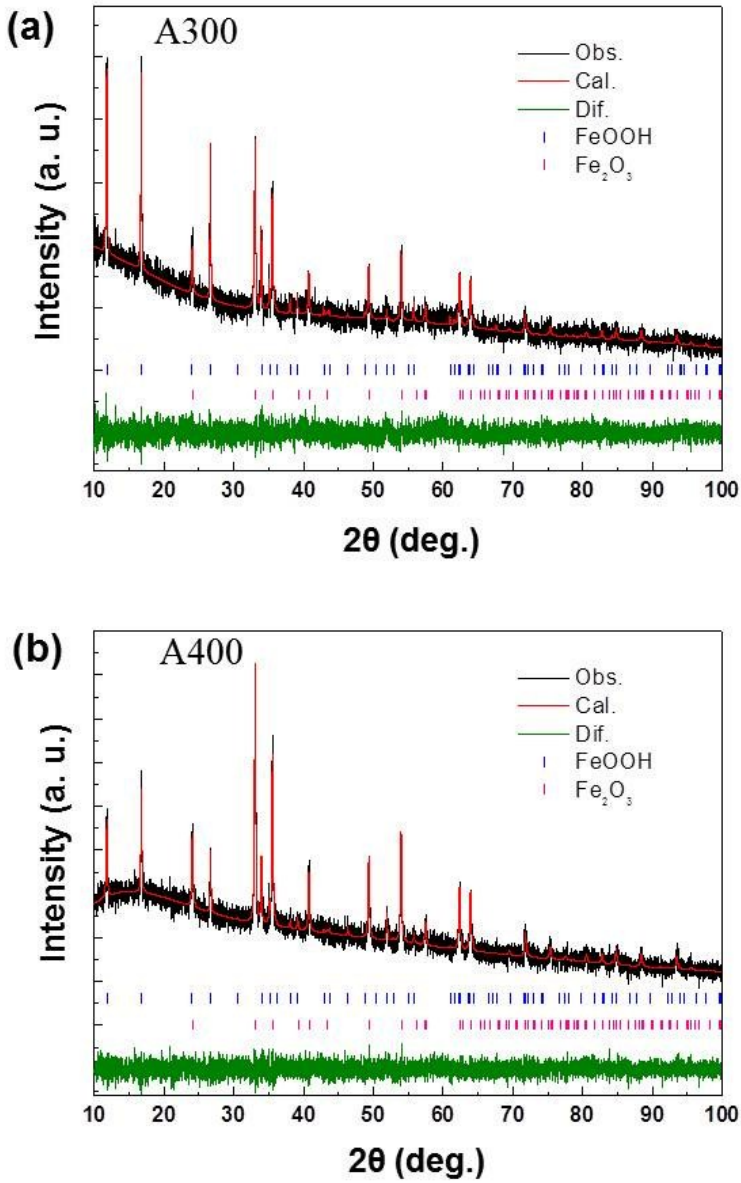

Fig. S19 Rietveld refinement patterns of A300 and A400 samples using X-ray powder diffraction data.